CrossMark

ORIGINAL ARTICLE

Investigation of interaction phenomena between crural fascia and muscles by using a three-dimensional numerical model

Piero G. Pavan[1,2] · Paola Pachera[1,2] · Antonella Forestiero[1,2] · Arturo N. Natali[1,2]

Abstract The focus of this work is the numerical modeling of the anterior compartment of the human leg with particular attention to crural fascia. Interaction phenomena between fascia and muscles are of clinical interest to explain some pathologies, as the compartment syndrome. A first step to enhance knowledge on this topic consists in the investigation of fascia biomechanical role and its interaction with muscles in physiological conditions. A three-dimensional finite element model of the anterior compartment is developed based on anatomical data, detailing the structural conformation of crural fascia, composed of three layers, and modeling the muscles as a unique structure. Different constitutive models are implemented to describe the mechanical response of tissues. Crural fascia is modeled as a hyperelastic fiber-reinforced material, while muscle tissue via a three-element Hill's model. The numerical analysis of isotonic contraction of muscles is performed, allowing the evaluation of pressure induced within muscles and consequent stress and strain fields arising on the crural fascia. Numerical results are compared with experimental measurements of the compartment radial deformation and intracompartmental pressure during concentric contraction, to validate the model. The numerical model provides a suitable description of muscles contraction of the anterior compartment and the consequent mechanical interaction with the crural fascia.

Keywords Crural fascia · Muscle · Constitutive modeling · Finite element analysis

1 Introduction

The deep fascia located in the human lower limb, known as crural fascia, creates three compartments, enwrapping and separating different groups of muscles [2, 21]. According to their location, it is possible to define an anterior, a lateral and a posterior compartment. In particular, the anterior compartment envelopes four muscles: tibialis anterior, extensor digitorum longus, extensor hallucis longus and peroneus tertius (when it is present). The lateral compartment includes the peroneus longus and brevis muscles; the posterior compartment contains the gastrocnemius and the soleus muscles, more internally, the popliteus, the flexor digitorum longus, the flexor hallucis longus and the tibialis posterior. Because of its composition, conformation and continuity [20, 21] crural fascia plays an important role in different aspects of leg biomechanics, being involved in muscle contraction coordination and load transmission.

Crural fascia can be described as a multilayer structure, composed of two dense connective tissue layers separated by an interposed loose connective tissue, and characterized by large content of hyaluronic acid with lubricating function [3]. Both the two dense layers are reinforced by collagen fibers mainly oriented along specific directions [21] and conferring mechanical anisotropic characteristics.

✉ Piero G. Pavan
piero.pavan@unipd.it

Paola Pachera
paola.pachera@unipd.it

Antonella Forestiero
antonella.forestiero@unipd.it

Arturo N. Natali
arturo.natali@unipd.it

1 Department of Industrial Engineering, University of Padova, Via Venezia 1, I-35131 Padova, Italy

2 Centre for Mechanics of Biological Materials, University of Padova, Via G. Marzolo 9, I-35131 Padova, Italy

Fig. 1 Fiber disposition from examination with polarized light reported with respect to the anatomical directions (proximal–distal, medial–lateral) and forming an angle α of about 74° (**a**). Stress–strain experimental curves from tensile tests on samples cut along longitudinal and transversal direction (**b**): for each direction, the minimum and maximum response (*gray lines*) and the average response (*black lines*) are reported
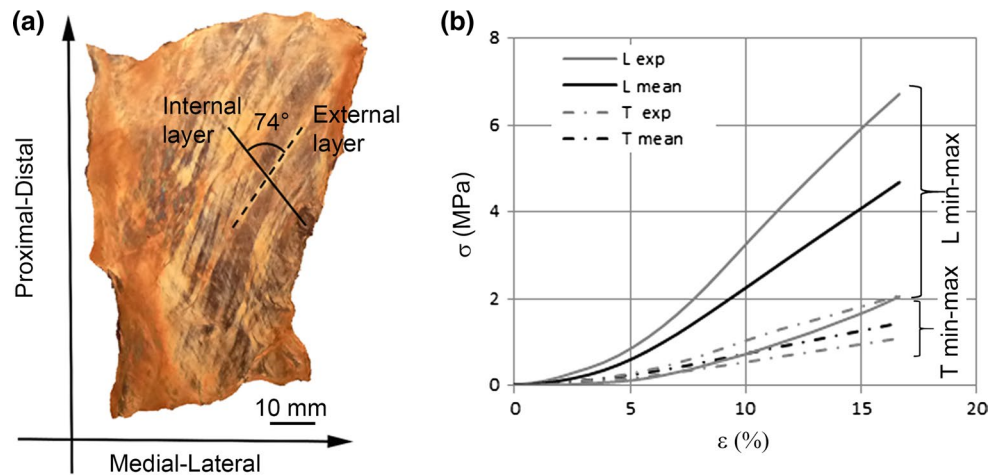
The knowledge about the biomechanical role of the crural fascia is limited, and few data about its mechanical properties can be found in the literature [5, 12, 18, 22]. This lack is also related to the high invasiveness required for the development of in vivo tests. To date, in vivo studies have focused on the evaluation of the intracompartmental pressures because of the clinical interest in the compartmental syndrome, whose etiopathology is not completely clear [11].

An attempt to boost knowledge on this area has been made by evaluating the intracompartmental pressure in different conditions, both on healthy and pathological subjects [8–10, 17, 24]. In a few cases, pressure measurements have been coupled with ultrasound measurements of the anterior compartment radial deformations [10].

In vitro tests are limited and main part of the tissues analyzed cannot be taken as representative of an average healthy condition because are usually dissected from elderly donors or from pathological subjects that have undergone amputation. As an additional limit, some experimental tests do not take into consideration the nonlinear mechanical behavior of the tissue and its anisotropic characteristics [5]. The literature shows also a limited investigation as regards the role of the crural fascia in force transmission, load transposition and related interaction with surrounding structures, such as bones. This aspect has been considered mainly from a qualitative point of view [14, 15], while a quantitative analysis is still absent.

All the aspects related to the fascia functional and biomechanical role are fundamental for a better understanding of several painful syndromes. A way of investigation can be found in the numerical modeling of this anatomical region, e.g., by means of finite element method (FEM). In a previous study by Dubuis et al. [6], a 3D FE model of a human leg is proposed to investigate the effects of an external pressure applied on the leg tissues. This work includes the analysis of the anterior region of the leg but does not account for the contractile properties of muscles.

In the present work, a three-dimensional FE model of the human anterior compartment is developed with attention to muscles and their interaction with crural fascia. The choice of modeling the anterior compartment is related to the large interest about clinical issues concerning this region, such as compartment syndrome.

This model represents an enhancement compared to previous analytical models [12] or two-dimensional numerical models [18]. It combines constitutive formulations capable of representing the anisotropic and nonlinear response of crural fascia and the contractile action of muscle tissues.

Numerical analyses are developed in order to investigate muscle–fascia interaction phenomena during muscle contraction and to evaluate the deformation fields induced on fascial tissues. Numerical outcomes are compared with experimental data from laser scanning of a leg both during rest condition and during maximal extension. Pressures within the compartment are also compared to those experimentally evaluated during concentric contraction [9], leading to a validation of the model.

2 Methods

2.1 Histological and experimental analyses

Experimental data on the crural fascia are taken from a previous study [22] made on three samples taken from a frozen adult donor (male, age 67, weight 74.8 kg, height 165.1 cm), corresponding to the leg medial third. The samples were first examined using polarized light in order to determine the distribution of fibers along the fascia. From the results of the image analysis, it was possible to confirm that the tissue is reinforced by two families of collagen fibers symmetrically disposed compared to the
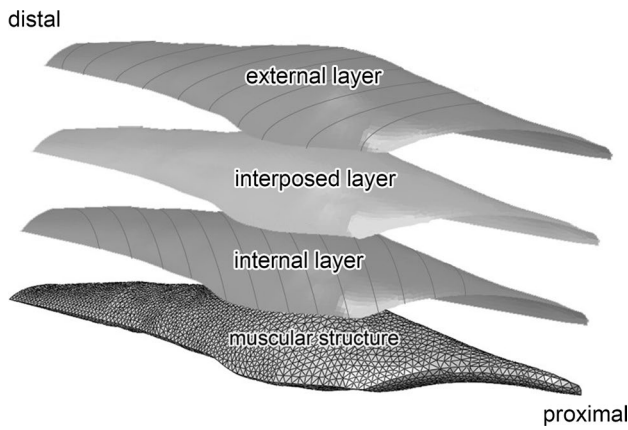
distal

external layer

interposed layer

internal layer

muscular structure

proximal

Fig. 2 Different regions of the anterior compartment numerical model: muscle structure and layers of crural fascia with the indication of fibers disposition

proximal–distal direction (Fig. 1a). Measures of the angle between fibers were performed on samples taken in different positions and showed a rather constant configuration, particularly in the central portion of fascia where the angle was around 74°. These experimental measurements are confirmed by data from the literature [21].

According to the symmetrical disposition of the fibers, mechanical tests refer to samples cut along the proximal–distal (longitudinal) and medial–lateral (transversal) directions [18]. Further details about the dissection and samples preparation are reported in [22]. Results from uniaxial tensile tests are reported in Fig. 1b, highlighting minimum, average and maximum responses for the two considered directions [22].

2.2 Solid and numerical modeling

The solid model of the anterior compartment consists in the crural fascia and the enveloped muscular structures. This is developed starting from MR images and accounting for histo-morphometric data in the literature [22]. According to histological data, the crural fascia is composed of three different layers: Two layers of dense connective tissue (mean thickness 0.3 mm) separated by a layer of loose connective tissue (mean thickness 0.2 mm). In the upper region, at the iliotibial tract, the crural fascia assumes a cone shape which represents the connection with the fascia lata of the thigh. Distally, at the height of the superior retinaculum, the thickness of the external layers is increased up to 0.55 mm for a width of about 30 mm, in order to reproduce the physiological thickening of the fascia observed experimentally. The muscular volume is surrounded externally by fascial components (Fig. 2) and, internally, by rigid surfaces representing the bounding of bones and interosseous membrane.

The numerical model is obtained by the FE discretization of the solid model by using CAE ABAQUS® software (SIMULIA, Dassault Systems). The external and the internal layers of the crural fascia are defined by four-node membrane elements, the interposed layer through hexahedral elements and the muscular structure discretized by tetrahedral elements (Fig. 2). Contact surfaces are defined between the inferior dense layer of the fascia and the enwrapped muscles. Null friction is considered to account for the condition of relative sliding between muscle and fascia.

A single volume is considered to account for the four muscles enwrapped by the crural fascia in the anterior compartment, with a pennation angle of 10°. The value is in the range (9.4°–13°) of the pennation angles characterizing these muscles [1]. To define the spatial disposition of the muscle fibers, a specific subroutine is implemented. The disposition of the fibers is specified at the level of each Gauss point of finite elements.

In order to evaluate the physiological shape variation due to the anterior muscular concentric contraction, the morphometry of the leg in a rest condition and during a maximal extension of the foot is considered. These two leg configurations are obtained starting from the acquisition of point clouds using the laser scanner FARO Edge ScanArm® (FARO Technologies, Inc., Lake Mary, FL).

2.3 Constitutive modeling

2.3.1 Constitutive formulation of crural fascia tissue

A fiber-reinforced and almost-incompressible hyperelastic constitutive model is assumed to interpret the biomechanical behavior of the layers of dense connective tissue [18]. This formulation is capable of describing large strains attained by the tissue, the presence of specifically oriented collagen fibers and the volume-preserving conditions induced by the high content of liquid phases, as assumed also for other connective tissues [4].

Defining the right Cauchy–Green strain tensor $\mathbf{C} = \mathbf{F}^T\mathbf{F}$, where $\mathbf{F}$ is the deformation gradient, the multiplicative decomposition in volume-changing and volume-preserving components $\mathbf{C} = J^{2/3}\mathbf{I} \cdot \tilde{\mathbf{C}}$ is considered, being $\mathbf{I}$ the second rank unit tensor and J the determinant of the deformation gradient. From the volume-preserving part $\tilde{\mathbf{C}}$ of the right Cauchy–Green strain tensor, the following modified invariants are obtained:

$$\tilde{I}_1 = \mathrm{tr}\left(\tilde{\mathbf{C}}\right), \quad \tilde{I}_4 = \tilde{\mathbf{C}} : (\mathbf{n}_0 \otimes \mathbf{n}_0) \tag{1}$$

being $\mathbf{n}_0$ a unit vector defining the local direction of collagen fibers in the undeformed configuration of the tissue.

The strain energy function W_f is defined as sum of two terms, W_{fm} for the ground matrix and W_{ff} for collagen

fibers that appoint local transversal isotropic properties to the single layer:

$$W_f = W_{fm} + W_{ff} = \left[\frac{\mu_f}{2}\left(\tilde{I}_1 - 3\right) + \frac{k_{fv}}{2}\left(J^2 - 1 - 2\ln J\right) \right]$$
$$+ \frac{\alpha_{f1}}{2\alpha_{f2}}\left[\exp\left(\alpha_{f2}\langle \tilde{I}_4 - 1 \rangle^2\right) - 1 \right] \quad (2)$$

where k_{fv} is related to the initial bulk modulus of the ground matrix, μ_f is its initial shear stiffness and α_{f1} (stress-like), α_{f2} (dimensionless) are constitutive parameters related to the mechanical response of the collagen fibers. The two family of collagen fibers are considered mechanically equivalent and are therefore characterized by the same values of the constitutive parameters. The fibers of the dense layers differ in terms of spatial orientation: The inner layer is characterized by fibers forming an average angle of 37° with the proximal–distal direction, while the external fibers are symmetrically disposed with respect to the proximal–distal direction. The stress response in terms of the first Piola–Kirchhoff stress tensor is obtained as $\mathbf{P} = 2\mathbf{F}\partial W_f / \partial \mathbf{C}$.

The fitting procedure refers to uniaxial tensile tests along proximal–distal and medial–lateral directions. These latter are recognized as the symmetric axes with respect to the initial fibers disposition. The constitutive parameters estimation is computed through the minimization of a scalar function expressing the error between experimental data and numerical results. The optimal values of the constitutive parameters are: 2000 MPa for k_{fv}, 0.6 MPa for μ_f, 4.88 MPa for α_{f1} and 3.61 for α_{f2}.

A hyperelastic neo-Hookean formulation is adopted for the interposed loose connective tissue, with a strain energy function W_l defined as:

$$W_l = \frac{\mu_l}{2}\left(\tilde{I}_1 - 3\right) + \frac{k_{lv}}{2}\left(J^2 - 1 - 2\ln J\right) \quad (3)$$

This layer is mainly composed of hyaluronic acid, which is usually regarded as a Newtonian fluid characterized by a constant viscosity of 5300 cP in a range of temperatures that includes 37 °C [19]. The assumption of Eq. (3) to describe the interposed layer response as elastic is based on the approximation that, during the analyzed muscle contraction, the interposed loose tissue is deformed at constant shear strain rate. The shear modulus μ_l is determined by means of the image analysis of an echographic video reproducing the mutual sliding of the dense layers of human fascia lata during thigh muscle contraction. Consequently, it is possible to compute the average sliding rate between selected points located in the different fascial layers. According to this datum and considering the thickness, a mean shear strain rate $\dot{\gamma}$ of 1.375 s^{-1} is computed for the interposed loose tissue

layer. Consequently, a shear modulus of 0.0017 MPa is calculated as $\mu_l = c\dot{\gamma}$.

2.3.2 Constitutive formulation of muscular tissues

The mechanical response of the muscles is described by a three-element Hill's functional model [16]. The model is characterized by two branches, one composed of a contractile element (CE) in series with a nonlinear spring (SE), and a second parallel branch with a nonlinear spring element (PE). The relationship between the stretch of muscle fiber λ_f, the stretch of the active part λ_m and the stretch of the passive part λ_s of sarcomeric elements is given by

$$(1 + k)\lambda_f = \lambda_m + k\lambda_s \quad (4)$$

where it is assumed $k = 0.3$, according to the literature. The stretch of the fiber is obtained as

$$\lambda_f = \sqrt{\tilde{\mathbf{C}} : (\mathbf{n}_0 \otimes \mathbf{n}_0)} \quad (5)$$

being $\mathbf{n}_0$ the unit vector representing the direction of the fiber in the undeformed configuration. The stress response of muscle tissue is defined as sum of isotropic $\mathbf{P}_{iso}$ and anisotropic $\mathbf{P}_{aniso}$ terms. The isotropic part is obtained via a standard derivation from a strain energy function of the form:

$$W_{iso} = \alpha_{m1} \exp\left[\alpha_{m2}\left(\tilde{I}_1 - 3\right)\right] + \frac{k_{mv}}{2}\left(J^2 - 1 - 2\ln J\right) \quad (6)$$

while the anisotropic part has a contribution of a passive term P_p and an active term P_a.

$$\mathbf{P}_{aniso} = \left(P_p + P_a\right)\mathbf{F}\mathbf{n}_0 \otimes \mathbf{n}_0 \quad (7)$$

The passive term is defined as

$$P_p = 4P_0\left(\lambda_f - 1\right)^2 \quad (8)$$

and is related to the response of the parallel elastic element PE. The active term given by the element CE is:

$$P_a = f_a(t)f_l(\lambda_m)f_v\left(\dot{\lambda}_m\right)P_0 \quad (9)$$

being P_0 the maximum isometric stress, assumed as 0.54 MPa, $f_a(t)$ the activation function, $f_l(\lambda_m)$ the force–length function, $f_v\left(\dot{\lambda}_m\right)$ the force–velocity function, t the time variable and $\dot{\lambda}_m$ the derivative of λ_m with respect to time.

The activation function is assumed in the form

$$f_a(t) = \begin{cases} a_0 & t \le t_0 \\ a_0 + (a_1 - a_0) \cdot h_t(t, t_0) & t_0 < t \le t_1 \\ a_0 + (a_1 - a_0) \cdot h_t(t_1, t_0) \cdot \left[1 - h_t(t, t_1)\right] & t_1 < t \end{cases}$$
$$(10)$$

where t_0 and t_1 are initial and final time instants of activation and the constants a_0, a_1 have been set as 0 and 1, respectively [13]. The function h_t is defined as:

$$h_t(t, t_i) = 1 - \exp\left[-S(t - t_i)\right] \tag{11}$$

with $S = 50 \text{ s}^{-1}$. The force–length function is assumed in the following form [7]:

$$f_l(\lambda_m) = \begin{cases} \dfrac{\lambda_m - \lambda_{min}}{\lambda_{opt} - \lambda_{min}} \exp\left[\dfrac{(2\lambda_{min} - \lambda_m - \lambda_{opt})(\lambda_m - \lambda_{opt})}{2(\lambda_{min} - \lambda_{opt})^2}\right] & \lambda_m > \lambda_{min} \\ 0 & \text{otherwise} \end{cases} \tag{12}$$

with $\lambda_{min} = 0.682$ and $\lambda_{opt} = 1.019$. The force–velocity function is described by a sigmoid shape:

$$f_v\left(\dot{\lambda}_m\right) = \frac{\delta_1}{\delta_2 + \delta_3 \exp\left(-\delta_4 \dot{\lambda}_m\right)} \tag{13}$$

assuming $\delta_1 = 1.514$, $\delta_2 = 0.996$, $\delta_3 = 0.542$ and $\delta_4 = 0.558$ s. The above relationship replicates the force–velocity function proposed by other authors [23]. Finally, the stress of the serial elastic element SE, which is always equal to the stress of the active element CE [7], is given by:

$$P_{SE} = \beta_0\left\{\exp\left[\beta_1(\lambda_s - 1)\right] - 1\right\} \tag{14}$$

having set $\beta_0 = 0.1$ MPa and $\beta_1 = 2.85$.

The constitutive model is implemented in the FE code by a user subroutine through an implicit integration scheme, exploiting the Eq. (4) and the equivalence $P_{SE} = P_{CE}$ to obtain the estimation of the stretches of SE, PE and CE elements at the current time.

2.4 Numerical analyses

The general-purpose FE code ABAQUS® (SIMULIA, Dassault Systems) is adopted for the numerical modeling proposed in this work. Different analyses are developed to test the reliability of the model both regarding the constitutive model of muscle tissue and the modeling of interaction phenomena of muscles with the crural fascia.

The constitutive model of the muscle is preliminary evaluated by simulating isometric and isotonic contractions of a muscle model with simplified geometry ending with two aponeuroses along the x-axis (Fig. 3). According to the symmetry of the structure, only one quarter of the structure is modeled. The contraction of the muscle is evaluated for two arrangements of the muscle fibers, in particular a disposition corresponding to a fusiform muscle and a disposition corresponding to a bi-pennate muscle with pennation angle of 30°. In the isometric contraction, the two ends of the structure are kept fixed in the direction of the muscle,
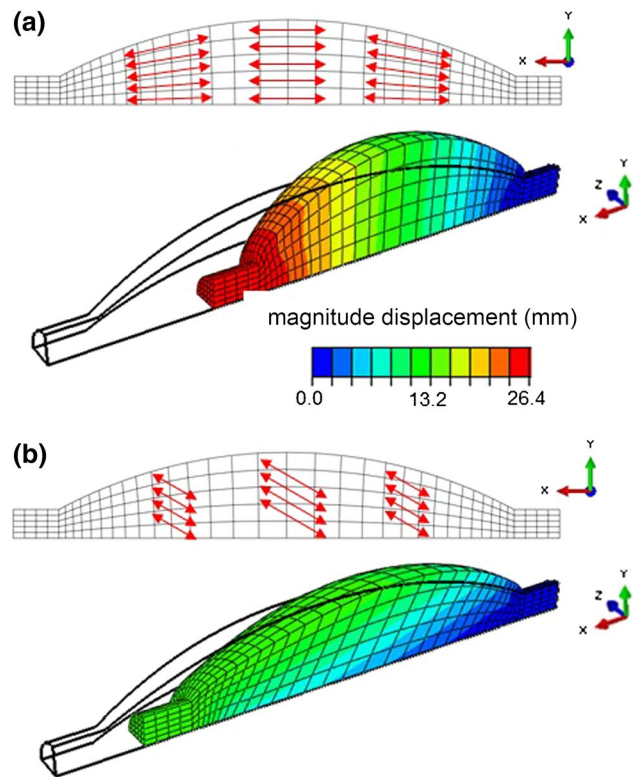

Fig. 3 Effects of muscle fibers disposition for an isotonic contraction at null imposed force in the case of fusiform muscle (**a**) and pennate muscle (**b**). Lower bulging and shortening are found in pennate muscle than in fusiform muscle

while this is activated. In the isotonic contraction, only one end is kept fixed, while the other end is free to move.

With regard to the numerical analysis of the anterior compartment, the extension movement is considered. The proximal extremity of the fascia is considered fixed. An isotonic contraction is applied simultaneously to the muscle fibers. This condition induces muscles shortening, as it occurs in an effective extension.

The validation of the numerical outcomes is performed by means of comparison with the experimental data at disposal. Laser scanning tests developed in this work on the anterior compartment at rest and at maximum extension allow to compare the deformation of this region in terms of radial displacements. These latter are computed by evaluating the variation of the distance between the skin surface and the bottom of the anterior compartment at the leg medial third. The distance is evaluated perpendicularly to the skin surface. The radial deformation (section B of Fig. 5) is here defined as $\overline{H'H''}/\overline{HH'} \cdot 100$. Further, experimental measurements of the intracompartmental pressure during contraction are taken from the literature to validate the numerical results.
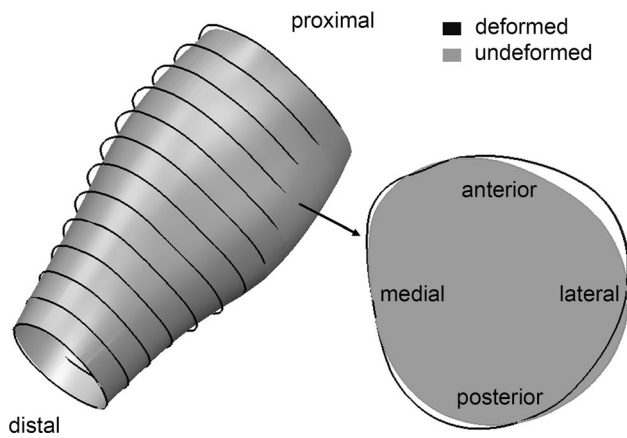
Fig. 4 Reconstruction by means of laser scanning of the leg external surface at rest condition (*gray*) with overlapping *black lines* corresponding to thirteen leg sections evaluated during the maximal extension. On the *right*, it shows the detail of a leg section

3 Results

Figure 3 shows the effect of muscle fibers spatial orientation in the case of isotonic contraction for the muscle with simplified geometry. The different behavior in the two cases is described by showing the respective magnitude displacement fields in the deformed configuration.

In Fig. 4, a comparison is made between the reconstruction performed using laser scanning acquisition of the external leg surface at rest condition (gray), with thirteen overlapping sections evaluated during the maximal extension (black lines). The comparison is made at the medial third section, evaluating undeformed and deformed shapes. Analogous comparison, obtained from the numerical model of the anterior compartment, is reported in Fig. 5 for the muscular structure. The contour of the magnitude of displacement component in the transversal plane is shown for two sections closed to the medial third region of the muscle. The maximum radial displacement is close to 5 mm in the upper section A, while it increases to 7 mm in the central section B.

By comparing the radial deformations obtained from numerical analysis and those evaluated by means of laser scanning, it is shown that the model well mimics the bulging. The maximum radial deformation is estimated as 15.2% in the numerical model and as 16.5% in the laser scanning acquisitions.

Figure 6a shows the magnitude displacement contour of the fascia internal layer for the whole structure. The displacement field of the internal layer shows values up to 7 mm; the maximum values are attained in the upper central portion of the structure. The same results are reported for the muscle structure (Fig. 6b) whose displacement field reaches values up to 43 mm in the distal region, being
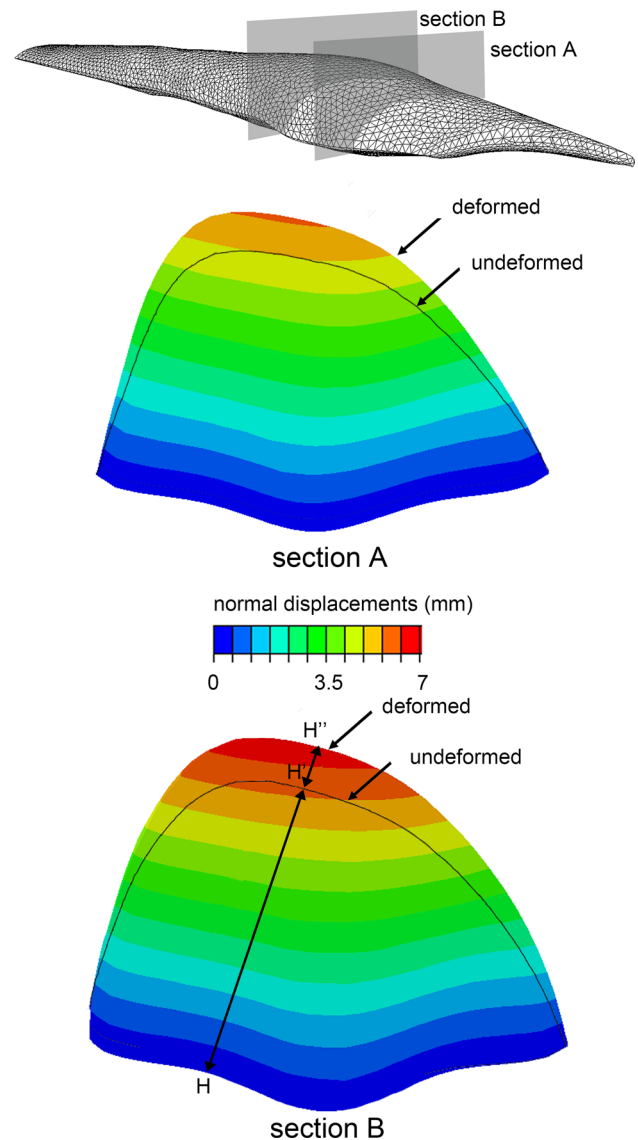

Fig. 5 Comparison between undeformed and deformed configurations of the muscle structure in two different transversal sections. The magnitude of displacement components in the transversal plane is also reported. Information about radial compartment measurement is highlighted in section B: the segment H–H′ represents the compartment radius in the undeformed configuration, and H–H″ is the compartment radius at the maximum muscle contraction

dominated by the displacement component along the distal–proximal direction.

Figure 7 reports the maximum principal stress in the internal and external layers of the fascia, showing an average value of about 1.5 MPa in the upper central region. The corresponding computed strain field (not reported in figure) shows values up to 16%. The tensile stress state of the crural fascia is in equilibrium with the internal pressure of the muscle compartment that is evaluated along a section at the medial third (Fig. 4, section A), finding an average pressure of 161.6 mmHg (21.5 kPa).
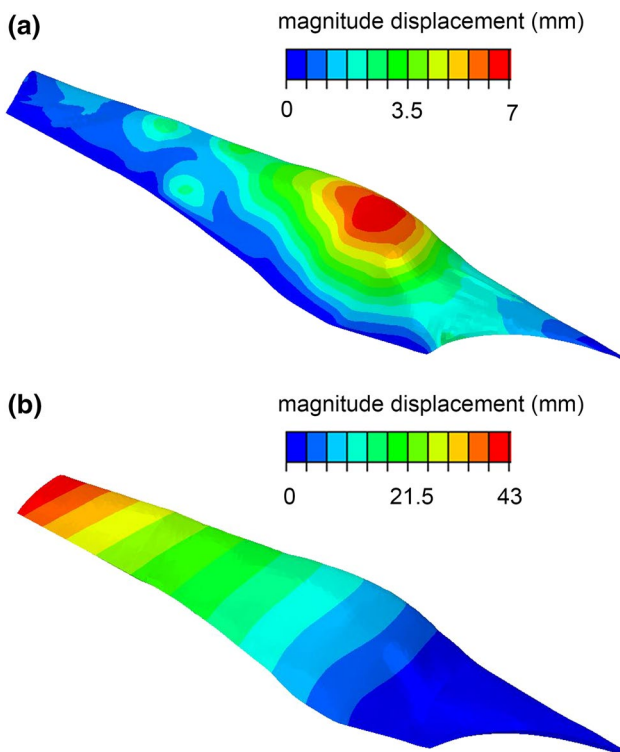
(a)

(b)

Fig. 6 Contour of the magnitude displacement in the internal layer of crural fascia (**a**) and in muscle (**b**)
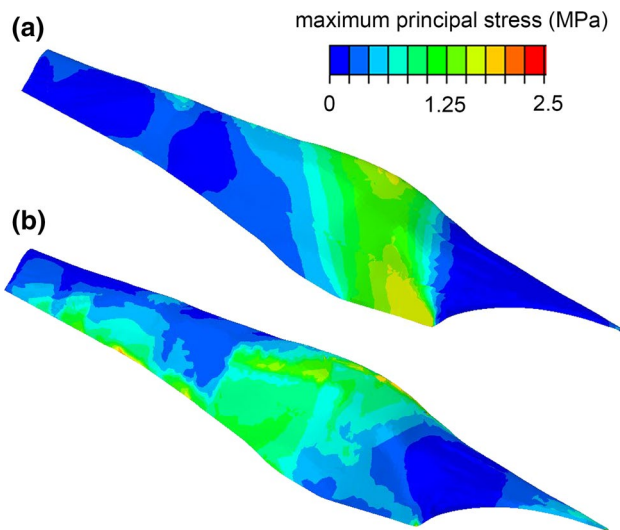
(a)

(b)

Fig. 7 Contour of the maximum principal stress in the internal (**a**) and external (**b**) layer of crural fascia

4 Discussion

Figure 3 shows the suitability of the constitutive model to represent the active behavior of muscle fibers for the simulated conditions. In the isotonic contraction with null external load applied, the fusiform muscles show a greater shortening due to the greater length of muscle fibers compared to the pennate muscle. The different deformation characterizing the two muscles is also evident, with a limited bulging of the pennate muscle compared to the fusiform one.

As pertain the analyses performed on the anterior compartment model, the numerical outcomes validation, previously assessed by comparison with laser scanning acquisitions, is strengthened by considering deformed configuration and pressure field resulting from the concentric contraction within the anterior compartment. The radial displacement computed in section A (Fig. 4) is comparable to that measured experimentally by ultrasound tests [10]. Further, Friden et al. [9] report intracompartmental pressure measurements on different subjects during concentric contraction, evaluated by means of catheters directly positioned in the upper portion of the anterior compartment, estimating a pressure of 157 ± 16 mmHg (20.9 ± 2.1 kPa). This value is closed to 161.6 mmHg (21.5 kPa) evaluated through numerical analyses.

The contour of the maximum principal stress (Fig. 7) highlights a stress distribution and orientation due to the different disposition of the fibers embedded in the two dense layers. This may reflect the physiological structural composition of the fascia highlighted by the histological analyses, characterized by two almost mutually independent and fiber-reinforced layers.

In the presented analysis of the anterior compartment, the force transmission between the internal fascia layer and the external surface of the muscle is not considered. This transmission could be given by connection of fibers between these structures, localized in the internal proximal region of the fascia. The density of these connections and their effect during the muscle contraction are difficult to quantify. Furthermore, very little is known about the real conformation of crural fascia connections and insertions in the upper and in the lower regions, at the height of knee and ankle joints, leading to a reasonable simplification of the model. The inclusion in the model of a region characterized by the connection of muscle fibers to the internal fascia layer will be possible by means of additional anatomical data and could provide a quantification of the force transmission between these structures.

The neglecting of time-dependent behavior of the crural fascia assumed in this work can be overcome by introducing a visco-elastic constitutive model for this tissue [22]. This would make it possible to account for different rates of activation of the muscle fibers. Such a refinement should also account for the effective viscous properties of the loose interposed layer of the crural fascia. The approximation made in this work appears reasonable according to the activation rate characterizing the simulated contraction and the specific experimental data of intracompartmental pressure taken as a reference [10].

The four muscles enwrapped by the crural fascia have been fused in a single region characterized by a similar disposition of fibers, considering a pennation angle within the range of the pennation angles that characterize muscles of the anterior compartment. In this way, the different origin and insertion of each muscle, its specific internal architecture, and the possibility of muscles independent activation are not considered. A possible enhancement could take into account the modeling of the muscles of the anterior compartment by means of four independent and mutually sliding regions, each described by a specific disposition of fibers, including the effective pennation angles. This simplification is assumed as a first attempt to investigate the effects of the extension, obtained by the contraction of all these muscles that are considered to act simultaneously.

Future developments will allow to account for other mechanical aspects related to different pathological conditions. As matter of example, it will be possible to simulate fascia herniation due to trauma or the effects due to fasciotomy and investigate the global mechanical changes in muscle–fascia system functionalities during contraction. Additional instigations will focused on fascia mechanics during muscle release after the contraction, to point out the role of the fascia as energy reserve during movement.

5 Conclusion

Despite the above-mentioned limitations, the model developed in this work represents a useful tool to evaluate the interaction between crural fascia and underlying muscular structures and to understand phenomena that are scarcely investigated through experimental practice. The proposed analysis supplies preliminary information about stress, strain and pressure magnitudes and distributions in a physiological state of extension. The comparison with experimental data at disposal shows that the model mimics correctly the biomechanics of the anterior compartment.

The model offers the possibility of analyzing further conditions. In particular, by changing loads and contact conditions between adjacent structures, it is possible to investigate different pathological scenarios. Interesting evaluations could be performed by reducing the mutual sliding between the internal and the external fascia layers or between the external fascia layer and muscle to assess the global mechanical changes. The quantification of the mechanical interaction phenomena could also be useful from a clinical point of view, to correlate biomechanical alterations to specific pathological cases.
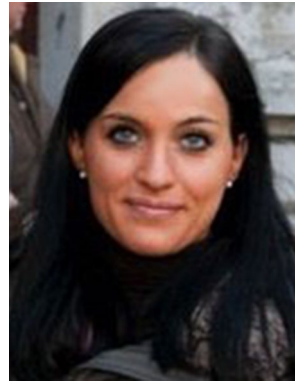
References

1. Arnold EM, Ward S, Lieber RL, Delp SL (2009) A model of the lower limb for analysis of human movement. Ann Biomed Eng. doi:10.1007/s10439-009-9852-5

2. Benjamin M (2009) The fascia of the limbs and back—a review. J Anat 214:1–18. doi:10.1111/j.1469-7580.2008.01011.x

3. Chaudhry H, Bikiet B, Roman M, Stecco A, Findley T (2013) Squeeze film lubrication for non-Newtonian fluids with application to manual medicine. Biorheology 50:191–202. doi:10.3233/BIR-130631

4. Cowin SC (2000) How is a tissue built? J Biomech Eng 122:553–569. doi:10.1115/1.1324665

5. Dahl M, Hansen P, Stål P, Edmundsson D, Magnusson SP (2011) Stiffness and thickness of fascia do not explain Chronic Exertional Compartment Syndrome. Clin Orthop Relat Res 469:3495–3500. doi:10.1007/s11999-011-2073-x

6. Dubuis L, Avril S, Debayle J, Badel P (2012) Identification of the material parameters of soft tissues in the compressed leg. Comput Methods Biomech Biomed Eng 15:3–11. doi:10.1080/10255842.2011.560666

7. Ehret A, Böl M, Itskiv M (2011) A continuum constitutive model for the active behaviour of skeletal muscle. J Mech Phys Solids 59:625–636. doi:10.1016/j.jmps.2010.12.008

8. French EZ, Price WH (1962) Anterior tibial pain. Br Med J 2:1290–1296

9. Friden J, Sfakianos PN, Hargens AR (1985) Muscle soreness and intramuscular fluid pressure: comparison between eccentric and concentric load. J Appl Physiol 61:2175–2179

10. Gershuni DH, Gosink BB, Hargens AR, Gould RN, Forsythe JR, Mubarak SJ, Akeson WH (2011) Ultrasound evaluation of the anterior musculofascial compartment of the leg following exercise. Clin Orthop Relat Res 10:59–65

11. Hargens AR, Schmidt DA, Evans KL, Gonsalves MR, Cologne JB, Garfin SR, Mubarak SJ (1981) Quantitation of skeletal-muscle necrosis in a model compartment syndrome. J Bone Joint Surg Br 63:631–636

12. Hurschler C, Vanderby R, Martinez DA, Vailas AC, Turnipseed WD (1994) Mechanical and biomechanical analyses of tibial compartment fascia in chronic compartment syndrome. Ann Biomed Eng 22:272–279

13. Joahansson T, Meier P, Blickhan R (2000) A finite-element model for the mechanical analysis of skeletal muscle. J Theor Biol 206:131–149. doi:10.1006/jtbi.2000.2109

14. Leonard J (2013) Importance of considering myofascial force transmission in musculoskeletal surgeries. J Surg Acad 3:1–3

15. Maas H, Sandercock TG (2010) Force transmission between synergistic skeletal muscles through connective tissue linkages. J Biomed Biotechnol. doi:10.1155/2010/575672

16. Mijailovich SM, Stojanovic B, Ko Liang A, Wedeen VJ, Gilber RJ (2010) Derivation of a finite-element model of lingual deformation swallowing from the mechanics of mesoscale myofiber

tracts obtained by MRI. J Appl Physiol 109:1500–1514. doi:10.1152/japplphysiol.00493.2010

17. Mubarak SJ, Owen CA, Hargens AR, Garetto LP, Akeson WH (1978) Acute compartment syndromes: diagnosis and treatment with the aid of the wick catheter. J Bone Joint Surg Br 60:1901–1905

18. Pavan PG, Pachera P, Natali AN (2015) Numerical modelling of crural fascia mechanical interaction with muscular compartments. Proc Inst Mech Eng H 229:395–402. doi:10.1177/0954411915584963

19. Roman M, Chaudhry H, Bukiet B, Stecco A, Findley TW (2013) Mathematical analysis of the flow of hyaluronic acid around fascia during manual therapy motions. J Am Osteopath Assoc 113:600–610. doi:10.7556/jaoa.2013.021

20. Stecco C, Porzionato A, Lancerotto L, Stecco A, Macchi V, Day JA, De Caro R (2008) Histological study of the deep fascia of the limbs. J Bodyw Mov Ther 12:225–230. doi:10.1016/j.jbmt.2008.04.041

21. Stecco C, Pavan PG, Porzionato A, Macchi V, Lancerotto L, Carniel EL, Natali AN, De Caro R (2009) Mechanics of crural fascia: from anatomy to costitutive modelling. Surg Radiol Anat 31:523–529. doi:10.1007/s00276-009-0474-2

22. Stecco C, Pavan PG, Pachera P, De Caro R, Natali AN (2014) Investigation of the mechanical properties of the human crural fascia and their possible clinical implications. Surg Radiol Anat 36:25–32. doi:10.1007/s00276-013-1152-y

23. Tang C, Zhang G, Tsui CP (2009) A 3D skeletal muscle model coupled with active contraction of muscle fibres and hyperelastic behavior. J Biomech 42:865–872. doi:10.1016/j.jbiomech.2009.01.021

24. Turnipseed WD, Hurschler C, Vanderby R (1995) The effects of elevated compartment pressure on tibial arteriovenous flow and relationship of mechanical and biomechanical characteristics of fascia to genesis of chronic anterior compartment syndrome. J Vasc Surg 2:810–817


Paola Pachera after M.Sc. in bioengineering got a Ph.D. in Industrial Engineering. Her research concerns soft tissue biomechanics, mechanical testing of biomaterials, constitutive and numerical modeling of biological structures.

Antonella Forestiero M.Sc. in bioengineering got a Ph.D. in Industrial Engineering. Her research concerns soft tissue biomechanics, constitutive and numerical modeling of biological structures with particular regards to foot biomechanics.

Piero G. Pavan is Associate Professor of Industrial Bioengineering with expertise in the field of hard and soft tissue biomechanics, mechanical testing of biomaterials, constitutive and numerical modeling of biological structures.
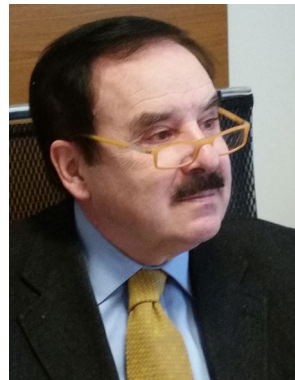
Arturo N. Natali is Full Professor of Industrial Bioengineering with research interests in biomechanics and bioengineering, including hard and soft tissue mechanics, constitutive and numerical modeling.